Visual response of posterior parietal neurons and saccadic reaction time during a visual detection task

Abbreviated title: Neuronal and behavioral performance during visual detection

Tomohiro Tanaka[1], Satoshi Nishida[1], Toshihiko Aso[2], and Tadashi Ogawa[1]

[1]Dept of Integrative Brain Science, Graduate School of Medicine, Kyoto University

Sakyo-ku 606-8501, Kyoto, Japan

[2]Human Brain Research Center, Graduate School of Medicine, Kyoto University

Sakyo-ku 606-8501, Kyoto, Japan

This is the pre-peer reviewed version of the following article: Visual response of neurons in the lateral intraparietal area and saccadic reaction time during a visual detection task. Eur J Neurosci. 2013 Mar;37(6):942-56, which has been published in final form at http://onlinelibrary.wiley.com/doi/10.1111/ejn.12100/abstract.

Corresponding author: Tadashi Ogawa, PhD

e-mail: togawa@brain.med.kyoto-u.ac.jp

Phone: +81-75-753-4678

FAX: +81-75-753-4486

Key words: stimulus intensity, response onset latency, saccadic reaction time, primate, visual salience

52 pages, 9 figures, 1 table

10365 words in whole manuscript, 231 words in Abstract, 474 words in Introduction

Abstract

Luminance is important in visual detection. A target with higher luminance is detected with reduced saccadic reaction times. However, little is known about how stimulus luminance affects the visual response in the posterior parietal cortex (PPC), and how luminance-related activity modulations are correlated with changes in reaction time. To address these issues, we recorded single-cell activity from visually responsive PPC neurons of monkeys required to make a saccade to an isolated target over five luminance levels. We found that as stimulus luminance increased, visual response strength increased, and response onset latency decreased. These luminance-related changes in activity were significantly correlated with changes in reaction time. Particularly, changes in response onset latency accounted for a substantial part of the observed changes in reaction time. However, the length of time from response onset to saccade onset was not constant but increased as luminance was reduced, suggesting the existence of other luminance-dependent processing in downstream and/or parallel pathways before saccade generation. Additionally, we failed to find strong covariance between response strength or latency and reaction time when the effect of luminance changes was removed. These results suggest that luminance-related changes in response strength and latency of PPC visual neurons may propagate to the saccade generation process, leading to substantial changes in reaction time. However, these response variables in the visual activity in PPC may contribute less directly to saccade generation itself during visual detection.

Introduction

Luminance is an important factor determining the detectability of visual stimuli. During detection of an isolated target with overt saccadic eye movements, saccadic reaction time generally decreases as the luminance of the target stimulus increases (e.g., Boch et al., 1984; Hughes and Kelsey, 1984; Marino and Munoz, 2009). Neurophysiological studies of visual areas have shown that greater luminance and contrast increase the strength of neuronal activity and reduce response onset latency (e.g., Gawne et al., 1996; Gawne, 2000; Lee et al., 2007).

The posterior parietal cortex (PPC), including the lateral intraparietal area (LIP), receives projections from many visual areas and is reciprocally connected with sites crucial for saccade generation such as the frontal eye field (FEF) and the superior colliculus (SC) (Andersen et al., 1990; Schall et al., 1995; Paré and Wurtz, 1997; Lewis and Van Essen, 2000; Ferraina et al., 2002). Many studies have shown that LIP plays important roles in various behavioral tasks requiring visuomotor transformations, such as target selection (Wardak et al., 2002; Ipata et al., 2006; Thomas and Paré, 2007, Balan et al., 2008; Ogawa and Komatsu, 2009), spatial attention (Gottlieb et al., 1998; Bisley and Goldberg, 2003) and motor planning (Snyder et al., 1997). Considering the anatomical and neurophysiological evidence, it is expected that luminance-related changes in the visual response of PPC neurons are associated with changes in saccadic reaction time. However, this possibility has not been systematically examined, although previous studies that examined this possibility in SC provided neuronal evidence supporting a link between SC visual response variables and saccadic reaction time (Bell et al., 2006; Marino et al., 2012).

To address this issue, single-cell activity was recorded from the region regarded as LIP while monkeys performed a visual detection task in which an isolated stimulus with five luminance levels was presented as a saccade target. These luminance levels were selected so that saccadic reaction time varied over a wide range. We examined how stimulus luminance affected the visual response of PPC neurons and how these response modulations were related to luminance-associated changes in saccadic reaction time. To investigate potential neuronal codes in the visual response of PPC neurons that could correlate with saccadic reaction time, we evaluated response onset latency and response strength measured in two ways: (1) post-latency strength (response strength immediately after the visual response onset) and (2) peak strength. As expected, luminance-related changes in these response variables of the visual activity in PPC were significantly correlated with changes in saccadic reaction time. In particular, changes in response onset latency accounted for a substantial part of the observed changes in saccadic reaction time. However, our additional analyses revealed that those response variables might contribute less directly to saccade generation. Thus, the present results suggest that the initial visual activity of PPC neurons plays a role as an intermediate factor in saccade generation during visual detection.

Materials and Methods

Animals and apparatus

Data were collected from two female macaque monkeys (*Macaca fuscata*; monkey Y: 4 years old, 5.0 kg; monkey S: 10 years old, 6.3 kg). Monkey Y was obtained from the National Bio-Resource Project (Aichi, Japan), and monkey S was from Nihon University (Tokyo, Japan). A plastic head holder and recording chambers were secured to the skull with dental acrylic resin (Unifast II, GC, Tokyo, Japan) and ceramic screws (Thomas Recording, Geissen, Germany). The recording chambers (22-mm inner diameter) were placed at stereotaxic coordinates (P0–4 and L18–21.5) above the intraparietal sulcus (IPS) with the assistance of magnetic resonance (MR) images acquired before surgery (see below). An eye coil was surgically implanted beneath the conjunctiva of one eye (Judge et al., 1980). The monkeys were allowed to recover for 2 weeks prior to training and recording. All procedures for animal care and experimental protocols were in accordance with the National Institutes of Health Guidelines for the Care and Use of Laboratory Animals (1996) and were approved by the Animal Care and Use Committee of Kyoto University.

The experiments were controlled by custom-made software on two Windows XP-based computers, which presented stimuli, recorded neural signals, and eye positions and controlled the task schedule. The software was developed using LabVIEW (National Instrument Japan, Tokyo, Japan) and C++ Builder (Borland Software Corporation, Scotts Valley, CA, USA). Visual stimuli were generated using a video-signal generator (ViSaGe; Cambridge Research Systems, Cambridge, UK) and presented on a video monitor with a

100-Hz refresh rate and 800 × 600 resolution (RDF223H; Mitsubishi, Tokyo, Japan). Stimuli were binocularly viewed from a distance of 42 cm in a dark room and subtended a visual angle of 51.5 × 40.0°.

Single neurons were recorded using an epoxylite-insulated tungsten electrode (Frederick Haer & Co, Bowdoinham, ME, USA) with an impedance >2 MΩ measured at 1 kHz (model IMP-1, Bak Electronics, Germantown, MD, USA). Extracellular activity was amplified using a microelectrode AC amplifier (Model-1800; A-M Systems, Carlsborg, WA, USA) and stored on a computer equipped with a multichannel analog-to-digital board at a sampling rate of 50 kHz (PCI-6143, National Instrument Japan). Eye position was monitored and recorded using the scleral search-coil technique (Fuchs and Robinson, 1966) (eye-position detector DSC-2001, Datel, Tokyo, Japan). Precise spikes were discriminated off-line using a template-matching method to confirm the method. Eye-position signals were recorded at a sampling rate of 50 kHz and analyzed at 1 kHz resolution.

The recording site was determined using a guide tube and a set of plastic grids with holes spaced 1.0 mm apart and offset from each other by 0.5 mm. The guide tube (23 gauge) was lowered above the dura matter surface, and the electrode penetrated the cortex through the dura using an oil hydraulic micromanipulator (MO-97A-S, Narishige, Tokyo, Japan). Under microscopic examination (OPMI-pico-i, Zeiss, Tokyo, Japan), a duratomy was performed using fine forceps (Dumont No. 5) and a 25-gauge needle with the tip bent at a right angle. Only a small region of the tissue just below the selected grid hole was removed to avoid breaking the electrode. The chamber was filled with agarose (3%, A9793; Sigma, St. Louis, MO, USA) to promote recording stability. After each recording session,

the dura matter surface was covered with anti-infective/anti-inflammatory ointment (Chlomy-P ointment, Daiichi-Sankyo, Tokyo, Japan).

Behavioral paradigms

Visual detection task. We analyzed the neural activity of 43 visually responsive PPC neurons obtained during this task. Each trial began with the onset of a fixation point (white circular spot, luminance = 66 cd/m^2) at the center of a monitor screen (Fig. 1). The monkeys had to fixate on that spot within a window of ±1.2–1.6°. After sustained fixation for a 1,000-ms or a 1,500–2,000-ms period, a circular target stimulus (size = 2.24°^{2}) appeared on a gray background. The target stimulus appeared with equal probability in the receptive field or in the location diametrically opposite the fixation spot. For each trial, the target luminance and position were selected in a quasi-random fashion. The monkeys were required to make a saccade to the target without an artificial delay (i.e., reaction-time task). When the computer detected a saccadic eye movement, the target and the fixation spot were immediately extinguished. If the monkey made a single saccade that landed inside a square target window surrounding the target (± 3.0 × 3.0°), another fixation point appeared at the target location. After fixation at this point for 600 ms, the monkey received a liquid reward (correct trial). If the gaze deviated from the fixation window before the target presentation, the trial was immediately aborted and the monkey did not receive a reward (aborted trial). In other situations, trials were considered erroneous and were grouped as follows: saccades landed outside the target window (saccade direction error); no saccade was made within a

1,200-ms interval after the target onset (no saccade error); and fixation broken during the secondary fixation after the saccade (post-saccade fixation error).

The target stimulus was presented at five luminance levels (0.83, 0.90, 1.02, 2.47, and 20.6 cd/m^2) for monkey Y and six luminance levels (0.80, 0.83, 0.90, 1.02, 2.47, and 20.6 cd/m^2) for monkey S on a background of uniform luminance (0.78 cd/m^2). The luminance levels were determined in an effort to create substantial variation in saccadic reaction times in response to changes in luminance. Only data that were obtained from the five shared luminance levels (0.83–20.6 cd/m^2) were used for analyses in the present study. They corresponded to 3.1%, 7.1%, 13.3%, 52.0%, and 92.7% contrast, calculated using the Michaelson formula, $(L_T - L_B)/(L_T + L_B)$, where L_T and L_B are the stimulus and background luminance. Because the target luminance was always brighter than the background luminance, only visual stimuli with positive contrasts were presented in this study. For easy comparison of the present results with previous ones, target luminance levels were also indicated by contrast. The eccentricity of the target was fixed at the 8.5° periphery to minimize inter-neuron differences in task difficulty across recording sessions because luminance or contrast sensitivity declines with retinotopical eccentricity in monkeys (e.g., Kiorpes and Kiper, 1996; Bell et al., 2000; Marino and Munoz, 2009) and in humans (e.g., Robson and Graham, 1981; Pointer and Hess, 1989; Foley et al., 2007). Furthermore, a recent study reported interaction effects between stimulus luminance and eccentricity on saccadic reaction time (Marino and Munoz, 2009).

Memory-guided saccade task. We used the memory-guided saccade task to assess visual and delay activity and to estimate the receptive field of a cell under study (Hikosaka and Wurtz, 1983). While the monkeys fixated on a central fixation point (yellow circle/square or white square spot, luminance = 56 or 66 cd/m^2), a single circular stimulus (luminance = 10 cd/m^2, size = 2.24°^{2}) was flashed for 500–700 ms. After a delay (900–1,800 ms) the fixation point was removed, and the monkeys were required to make a saccade to the location of the previously flashed target. The other procedures for this task were similar to those for the visual detection task.

Data collection

Single-cell activity was recorded by advancing an electrode into the lateral bank of IPS, as verified by structural magnetic resonance imaging (MRI) before the start of recordings. Once a neuron was isolated during recording sessions, we initially assessed the location of the receptive field in the memory-guided saccade task. An isolated stimulus was presented at one of six evenly separated directions on an imaginary circle (eccentricity = 8.5°), because the target-location eccentricity was fixed at 8.5° in the periphery during the visual tasks, and because the preferred directions of LIP neurons are invariant regardless of the target eccentricity (Barash et al., 1991b). We determined the preferred direction by manually adjusting those six directions so that one direction evoked the strongest activity. After that, we conducted the visual detection task by presenting the target in either the preferred direction (within the receptive field) or the opposite direction (outside the receptive field). If the neuron remained well isolated after the recording in the visual

detection task, we recorded from the same neuron when the monkey performed the memory-guided saccade task. We were able to record neuronal activity from 35 of 43 cells studied.

Before starting the present experiment, we specified the IPS location based on response properties; the medial bank of IPS tends to exhibit activity related to somatosensory stimuli, whereas the lateral bank exhibits visual and saccade-related responses (Mountcastle et al., 1975; Barash et al., 1991b; Maimon and Assad, 2006). After specifying the IPS locus, we recorded neurons in the lateral bank of the IPS, from a region regarded as LIP, in which neurons exhibit robust, spatially tuned responses during the delay period of a memory-guided saccade task (Gnadt and Andersen, 1988; Barash et al., 1991a, b; Colby et al., 1996; Shadlen and Newsome, 2001). To ensure that our samples were in area LIP rather than area 7a, neurons recorded at a depth shallower than 3 mm from the dura surface were excluded from the present analysis (Andersen et al., 1990; Linden et al., 1999; Gifford and Cohen, 2004). Neurons were typically recorded at >5-mm depth from the dura surface (88%), and the majority of our observed neurons (62.9%, see Results) exhibited significant modulations in delay-period activity (determined by whether activity 150–650 ms after target offset differed significantly according to target location; Mann–Whitney *U*-test, $p < 0.05$; Lawrence et al., 2005). This fraction was comparable to that reported for LIP in previous studies (e.g., Barash et al., 1991a; Maimon and Assad, 2006; Falkner et al., 2010).

To verify the recording positions, we acquired post-operative structural MR images for both monkeys on a 0.2 Tesla open whole-body scanner (Signa Profile; General

Electric, Milwaukee, WI, USA). The advantage of this low-magnetic field system is reduced distortion of the original cortical structures (Petersch et al., 2004). We used a three-dimensional spoiled, gradient-recalled (SPGR) pulse sequence with the following parameters: TR = 29 ms, TE = 8.3 ms, flip angle = 40°, field of view = 16 cm, 256 × 256 matrix, 100 slices, voxel size = 0.63 × 0.63 × 1.0 mm). To improve the image signal-to-noise ratio, we aligned and averaged two or three acquisitions during post-processing. Figure 2 shows MR images from one monkey (monkey Y). We used five plastic hollow tubes filled with an 84–87% glycerin solution (Glycerin P, Kenei, Tokyo, Japan), which were visible in the MRI, to determine the plane and trajectory of the electrode penetrations (Fig. 2A). These tubes were embedded in a plastic base attached to the recording chamber so that one was the center and the remaining four were arranged in the x–y coordinate (8 mm apart from the center) of the recording grid (Fig. 2B). The penetration sites on the brain surface were reconstructed based on the coordinates determined by the positions of the reference tubes. Figure 2D shows the MR images that matched the plane of the recording penetrations. The zone of the recording sites (arrow heads), which was reconstructed from a combination of grid sites and recording depths, is superimposed on the MR images. Figure 2C shows a number of neurons recorded within each grid location, and Figure 2E shows coronal slices representing recording positions from the most anterior to the most posterior. Thus, our samples were presumably recorded from LIP based on the physiological properties of the recorded neurons and verification by the MR images. However, we did not histologically reconstruct the precise recording sites,

as the monkeys are still alive and are to be used for other studies. For this reason, we will use the term “PPC” to indicate the region from which we recorded.

Data analysis

Only correct trials were analyzed. Spike density functions were constructed with 1-kHz resolution by convolving spike trains with a Gaussian function (SD = 3 ms) (Richmond et al., 1987). Population average spike density functions were constructed by averaging the spike density functions from individual neurons for each luminance condition. Eye velocity was calculated by digitally distinguishing between eye-position signals. Saccades were detected using a computer algorithm that identified the initiation and termination of each saccade based on a velocity-threshold criterion. Change in eye velocity was recognized as a saccade if it was greater than the threshold of 120°/s for at least 10 ms. The initiation of a saccade was defined as the time at which the velocity increased to >30°/s, and the saccade offset was defined as the time at which the velocity fell to <30°/s. Saccadic reaction time in the visual detection task was defined as the interval from the appearance of the target to the initiation of the saccade. Saccade duration was defined as the time from the saccade onset to offset, and saccade endpoint error was defined as the distance between the saccade endpoint and the target position. We excluded the trials that had unusually short or long saccadic reaction times (more than 2 SDs above or below the mean saccadic reaction time for correct trials for each trial condition; on average, 5.5% of trials were discarded).

Visual responsiveness was determined using the following two criteria: (1) the activity at 50–150 ms after the target onset was significantly greater than the activity at

200-ms prior to the target onset during the memory-guided saccade task (two-tailed *t*-test, $p < 0.01$); and (2) the visual response onset preceded the mean time of saccade onset by at least 50 ms for all luminance conditions during the visual detection task. For eight of 43 cells, neuronal data during the memory-guided saccade task were not stored. However, because visually responsive activity was confirmed by on-line observation when we determined the preferred target direction using the memory-guided saccade task, these cells were included in the data analysis.

To investigate potential neuronal codes that could be correlated with saccadic reaction time in the visual response of PPC neurons, we considered response onset latency and response strength, and examined the correlation between these response properties and saccadic reaction time. Response onset latency was determined using a Poisson distribution analysis (Maunsell and Gibson, 1992; Bisley et al., 2004; Price et al., 2006; Crowder et al., 2009). The baseline activity in the 200 ms immediately prior to stimulus onset for all luminance conditions was fitted with a Poisson distribution. A threshold was then calculated based on a 99% cutoff from the fitted distribution ($p < 0.01$). Response onset latency was defined as the time point following the onset of the stimulus when the spike density function exceeded this threshold and stayed above the threshold for 5 ms. For seven out of 43 cells, because the response onset latency was undetermined at the 99% threshold level, it was calculated at the 95% threshold level ($p < 0.05$).

Two types of response strength were determined using the following two criteria. (1) *Post-latency strength*: mean strength during the 50-ms period immediately after visual response onset. This measurement quantified the strength of the initial visual response

irrespective of response onset latency (Gawne, 2000; Lee et al., 2010). It was unlikely that the effect of the saccade related activity substantially invaded the analyzed period because the response onset preceded the mean time of the saccade onset by more than 50 ms (mean = 98.0 ms, range 50.6–217.8 ms). (2) *Peak strength*: Peak activity was defined as activity occurring at the first time point at which the activity was maximum within the preceding and subsequent 10-ms periods after it exceeded 2 SDs from the mean baseline activity. To avoid erroneous detections due to minor activity fluctuations, we first detected the peak activity time by moving the time point in 1-ms steps on the spike density function constructed with a Gaussian function (SD = 10 ms). Then, for precise determination, we re-detected the peak activity time within the 5-ms interval of the previously detected peak-strength time using the spike density function constructed with a Gaussian function (SD = 3 ms). If such peak activity was not detected in the interval from the response onset to the saccade onset, the maximum firing rate within that period was used as the peak activity (n = 3, 1, 1, 1, and 6 at stimulus luminance of 20.6, 2.47, 1.02, 0.90, and 0.83 cd/m^2, respectively).

To estimate the confidence intervals for response strength and response onset latency, we used a bootstrap analysis for each stimulus condition for each neuron (Efron and Tibshirani, 1993). To generate a new bootstrap sample, we randomly sampled, with repetition, trials from the original data set until the new set had the same number of trials as the original. The response strengths and response onset latencies were calculated in the same way as the actual data. This procedure was followed for 2,000 iterations, and then 95% confidence intervals of the distributions were estimated.

Results

Behavioral performance

In the visual detection task, the monkeys were required to detect a target and indicate the target's appearance by shifting their gaze to the target location (Fig. 1A). Figure 1B shows the average number of correct performances obtained from 43 recording sessions. The result was calculated from both trials when the target appeared in the receptive field and those when it appeared outside the receptive field. The monkeys performed well, with >95% correct response trials at all five luminance levels. Across all luminance levels, the rate of erroneous trials was 2.4%. Erroneous trials could be classified into three types (see Materials and Methods): saccade direction error (53.5%), no saccade response within 1,200 ms after stimulus onset (4.9%), and post-saccade fixation error (41.6%). Figure 1C shows mean saccadic reaction times across recording sessions as a function of luminance. As the luminance increased, saccadic reaction time decreased. This was consistent with previous studies (Boch et al., 1984; Hughes and Kelsey, 1984; Doma and Hallett, 1988; Jaśkowski and Sobieralska, 2004; Marino and Munoz, 2009). When luminance increased from darkest (0.83 cd/m^2) to brightest (20.6 cd/m^2), mean reaction time decreased by 89 ms, suggesting that the range of luminance used in the present study was sufficient to modulate target detectability in the visual detection task.

The dependence of saccade dynamics on stimulus luminance is summarized in Table 1. As a trend, we found increased saccade peak velocity and amplitude as well as decreased saccade duration as stimulus luminance increased. Although these changes were significant (one-way repeated-measures analysis of variance [ANOVA], $F_{4,168}$ = 132.8 for

peal velocity, $F_{4,168}$ = 13.6 for amplitude, and $F_{4,168}$ = 29.4 for duration, $p < 0.001$), the absolute magnitude of these changes was rather small (5.5% for peak velocity, 1.2% for amplitude, and 6.1% for duration).

Visual responses to stimuli of differing luminance

We recorded the activity from 89 cells in the region regarded as LIP during the visual detection task. For 61 of those neurons, the data sets were large enough to enable analysis (≥20 trials for each of the stimulus conditions: five luminance levels × two target positions). Of these, 43 cells (21–125 trials, mean ± SD = 34 ± 15.1 trials; n = 31, monkey Y; n = 12, monkey S) fulfilled the criteria for visually responsive activity and were further analyzed in this study. Thirty-five of these cells were also examined in the memory-guided saccade task, and 22 (22/35 = 62.9%) had significant delay-period activity. Because the results were essentially the same when the data from neurons with and without delay-period activity were separately analyzed, we show the results of the analysis performed on the combined data from all neurons.

Figure 3 shows spike density functions (mean ± SEM) from the five luminance levels of a PPC neuron. Each trace was calculated from 30–35 success trials. The initial visual activity exhibited clear elevations after stimulus onset. Squares indicate the times at which response onset latencies were assigned. As shown in the figure, response strength substantially varied associated with changes in stimulus luminance (middle panel in Fig. 3B). To provide insight into how this neuron encoded changes in stimulus luminance by its response strength, we calculated trial-averaged post-latency strength (Fig. 4A) and peak

strength (Fig. 4B). As a general trend, this cell exhibited an increase in post-latency and peak strengths as stimulus luminance increased, although post-latency strength did not increase monotonically with the increase in luminance. Furthermore, changes in stimulus luminance also affected response onset latency (left panel in Fig. 3B). As shown in Fig. 4C, response onset latency clearly decreased in a monotonic fashion with the increase in luminance.

Luminance dependence of population average responses

To determine whether the response profiles illustrated in the example neuron (Figs. 3 and 4) were preserved in the population average response, the spike density functions obtained from 43 PPC neurons were averaged across all neurons (Fig. 5). As target luminance increased, in general, response strength increased (middle panel in Fig. 5) and response onset latency decreased (left panel in Fig. 5). The right panel of Fig. 5 shows the population responses aligned at the saccade onset. Shadlen and coworkers reported that when monkeys made gradual decision formation during a discrimination task, the activity of LIP neurons (they only examined neurons with delay-period activity in a memory-guided saccade task) tended to exceed a common threshold level prior to the generation of saccades (Roitman and Shadlen, 2002; Gold and Shadlen, 2007). However, our samples did not show a clear common activation level. The magnitude of pre-saccadic strength (the mean discharge rate measured 10–20 ms prior to the saccade onset) was significantly different across the different luminance levels (one-way repeated-measures ANOVA, $F_{4,168} = 4.96$, $p < 0.001$). This was true even when the neuronal population was restricted to the

neurons that had significant delay-period activity (n = 22; one-way repeated-measures ANOVA, $F_{4,84} = 4.0$, $p < 0.01$).

Luminance-dependent changes in response strength and response onset latency

To illustrate how individual PPC neurons encoded changes in stimulus luminance in their response strength, we calculated post-latency and peak strengths at the five luminance levels for each neuron (Fig. 6A and B). Each response strength was normalized so that the mean value across the five luminance levels of each neuron was 1 so that data would not be more affected by neurons with greater response strength. There were significant increases across neurons in both normalized post-latency strength (Fig. 6A, Pearson correlation test, r = 0.48, $p < 0.001$, the degrees of freedom [df] = 213) and normalized peak strength (Fig. 6B, Pearson correlation test, $r = 0.55$, $p < 0.001$, df = 213) associated with the increase in stimulus luminance. However, at the individual neuron level, there were substantial fluctuations in the representation of luminance (gray circles and lines). Only in a few neurons, the increase in luminance was monotonically encoded by the increase in post-latency strength (14% = 6/43) and peak strength (14% = 6/43).

Figure 6C shows the relationship between response onset latency and stimulus luminance. There was a significant and strong correlation across neurons between response onset latency and luminance (gray line, r = -0.77, $p < 0.001$, df = 213). Mean response onset latencies were 63.9 ± 13.2 (mean ± SD), 70.9 ± 11.8, 88.3 ± 16.7, 95.9 ± 16.1, and 122.6 ± 20.6 ms for target luminance of 20.6, 2.47, 1.02, 0.90, and 0.83 cd/m^2, respectively. Thus, response onset latency monotonically decreased as stimulus luminance increased. In

contrast to response strength, many neurons (86% = 37/43) monotonically encoded stimulus luminance in their response onset latencies at the individual neuron level. These results indicate that the strength and the onset latency of visual response significantly changed in association with changes in stimulus luminance. Particularly, response onset latency was capable of representing stimulus luminance using a monotonic encoding strategy.

Relationship between response strength/response onset latency and saccadic reaction time

We then examined the relationship between luminance-related modulations in the initial visual response of PPC neurons and changes in saccadic reaction time at the population level. Figure 7, A and B shows the relationship between normalized post-latency strength/peak strength and saccadic reaction time. The reduction in both normalized post-latency and peak strengths for 43 neurons was mildly correlated with the increase in saccadic reaction time (Fig. 7A, Pearson's correlation test, $r = -0.42$, $p < 0.001$, df = 213; Fig. 7B, $r = -0.51$, $p < 0.001$, df = 213). For individual neurons, the strength of the correlation (r) of normalized post-latency strength with saccadic reaction time ranged from -0.993 to 0.842 (median = -0.717, mean ± SD = -0.481 ± 0.571), and that of normalized peak strength ranged from -0.980 to 0.732 (median = -0.650, mean ± SD = -0.506 ± 0.502), indicating substantial variance in the relationships of both normalized post-latency and peak strengths with saccadic reaction times across neurons.

Figure 7C shows the relationship between response onset latency and saccadic reaction time. Luminance-related changes in response onset latency for 43 neurons were more strongly correlated with changes in saccadic reaction time (Pearson's correlation test, $r = 0.76$, $p < 0.001$, df = 213) than were changes in post-latency and peak strengths. Even at the individual neuron level, the correlation values were high for all neurons (range: 0.850–0.999; median = 0.970, mean ± SD = 0.958 ± 0.04). Thus, strong correlations between response onset latency and saccadic reaction time were observed across neurons. However, despite such strong correlations, our results also showed that changes in response onset latency did not fully account for changes in saccadic reaction time. When stimulus luminance decreased from 20.6 to 0.83 cd/m^2, saccadic reaction time of trials in which the target appeared in the receptive field was prolonged by 94.8 ms (from 148.8 to 243.6 ms) on average, but response onset latency lengthened by only 58.7 ms (from 63.9 to 122.6 ms), indicating that although luminance-related changes in response onset latency explained a substantial part (61.9% = 58.7/94.8) of the total change in saccadic reaction time, this explanation was not complete. To understand how stimulus luminance affected the length of time from visual response onset to saccade onset, we calculated the neuronal–saccade onset delay for each of the luminance levels (Fig. 8). The results showed that the delay time was not constant (one-way repeated-measures ANOVA, $F_{4,168} = 43.9$, $p < 0.0001$) but instead tended to gradually increase as stimulus luminance decreased. Such a systematic luminance dependency in the neuronal–saccade onset delay suggests that other luminance-dependent processes contribute to saccade generation and that the response onset latency of PPC neurons contributes less directly to saccade generation.

Covariation analysis of response onset latency and saccadic reaction time

As described above, it is unlikely that there is a rigid link between response onset latency and saccadic reaction time. To asses this in a more direct way, we conducted a covariation analysis that was similar to a method previously utilized (e.g., Thompson et al., 1996; Sato et al., 2001; Ipata et al., 2006; Thomas and Paré, 2007). This analysis allowed us to examine the relationship between response strength/response onset latency and saccadic reaction time under the condition in which the effects of luminance changes were removed. We first examined the relationship between the variability in response strength (normalized post-latency and peak strength) and that in saccadic reaction time (Fig. 9A and B). For each neuron, trials under each luminance condition were divided into two equal-sized groups according to saccadic reaction time (short vs. long reaction-time groups), and mean normalized post-latency/peak strength was computed for both reaction-time groups. Figure 9A shows the difference in mean normalized post-latency strength for the two reaction-time groups as a function of the difference in mean saccadic reaction times for the two groups. Each data point indicates one of the five luminance levels for each neuron. Six of the total data points (n = 215; 5 luminance levels × 43 neurons) were excluded from this analysis, because post-latency strength was not defined due to the undetection of response onset latency with a 95% cutoff from the Poisson distribution. The slope of a regression line, which was forced to pass through the origin, was not significantly different from zero (regression slope = -0.00052, $p > 0.05$, df = 207), indicating that there was no covariance between the two variables. Similar non-significant covariance was observed between

normalized peak strengths and saccadic reaction times (Fig. 9B; regression slope = -0.00061, $p > 0.05$, df = 213). Thus, the variability in measures of response strength in this study did not account for the variability in saccadic reaction times when the effects of luminance changes were removed.

Next, we examined the relationship between the variability in response onset latency and that in saccadic reaction times. Six data points were excluded from this analysis for the same reason described in Fig. 9A. In contrast to measures of response strength, there was a significant correlation between variability in response onset latencies and variability in saccadic reaction times (Fig. 9C; regression slope = 0.10, $p < 0.01$, df = 207). However, the slope of the regression line was very small. The deviation of data points in the bottom-right direction from a diagonal line (dashed line) indicated that changes in response onset latencies were smaller than those in saccadic reaction times. This result was consistent even when the analysis was conducted separately on the datasets for each luminance level (Fig. 9D). The slope of the regression line was positive for either luminance level, although the slope values were not significantly different from zero for all luminance levels (regression slopes = 0.028–0.15, $p > 0.05$, df = 38–41). Taken together, the results of the covariation analysis revealed that variability in no response property (i.e., post-latency strength, peak strength, response onset latency) was capable of accounting for a major part of the variability observed in saccadic reaction times.

Discussion

We found that the majority of visually responsive PPC neurons significantly changed their activity associated with changes in stimulus luminance. On average, luminance-related changes in response strength (post-latency and peak strength) and response onset latency were significantly correlated with changes in saccadic reaction time. In particular, response onset latency was strongly correlated with saccadic reaction time. However, the time from the response onset to the saccade onset was not constant but increased as luminance was reduced, suggesting that other luminance-dependent processing may lie downstream and/or in parallel circuits and contribute to the timing of saccade generation. Additionally, there was no strong correlation between the variability in response onset latency and the variability in reaction times when the effects of luminance changes were removed. Based on these findings, we will discuss the role of PPC in single-target detection and saccade generation during visual detection.

Comparisons with previous studies of response onset latency

To our knowledge, there have been no systematic studies of the dependence of response onset latency on stimulus luminance in LIP. Neuronal activity was examined using one particular luminance level (e.g., Barash et al., 1991a; Bisley et al., 2004). Therefore, we selected a contrast level in our study that matched the stimulus contrast used in a previous study by Bisley et al. (2004) to make a comparison. They precisely determined response onset latency using a Poisson distribution analysis and showed that mean response onset latency for 41 LIP neurons was 49.5 ms (range: 42–76 ms) for a

stimulus with 55% contrast. In our case, mean response onset latency was 70.9 ms (range: 55–106 ms) for a stimulus with 52% contrast. Although the distribution ranges substantially overlapped, the mean response latencies differed. One possible explanation is that this difference was due to the lower luminance of the target and background used in the present study as compared with those used in the previous study.

Schmolesky et al. (1998) gathered response onset latency data from many brain areas of anesthetized monkeys using a stimulus with 80% contrast. They showed that mean latencies (±SD) of neurons in areas associated with the dorsal stream of visual processing were rather uniform across areas: V3 (72 ± 8.6 ms), the middle temporal area (72 ± 10.3 ms), the medial superior temporal area (74 ± 16.1 ms), and FEF (75 ± 13.0 ms), indicating that dorsal stream signals rapidly traverse to higher levels of the anatomical hierarchy. The response onset latency reported here (70.9 ± 11.8 ms for a stimulus with 52% contrast) was comparable to that of those areas. In contrast, this latency was shorter when compared with those in areas associated with ventral pathways such as areas V4 (104 ± 23.4 ms) (Schmolesky et al., 1998) and TE (151 ± 50 ms) (Nakamura et al., 1994). Therefore, visual signals from ventral-stream areas (Andersen et al., 1990; Blatt et al., 1990; Lewis and Van Essen, 2000) are unlikely to explain the response onset latency observed in our sample. Thus, the present result provides functional evidence supporting that the initial visual response of PPC neurons may be signaled through dorsal-stream areas that are connected with LIP (Andersen et al., 1990; Blatt et al., 1990; Lewis and Van Essen, 2000).

A potential role of response onset latency in the formation of a saliency map

We found the robust monotonic dependence of response onset latency on stimulus luminance (Fig. 6). This monotonic coding may play a crucial role not only in visual detection but also in visual search. Theoretical models of attention (Koch and Ullman, 1985; Wolfe, 1994; Itti and Koch, 2000) suggest that the brain has a single map that represents the stimulus-driven conspicuity of individual objects (*salience map*). It is generally accepted that a salience map is represented by a network spanning over multiple areas; LIP is one of those areas (Bisley and Goldberg, 2003; Ogawa and Komatsu, 2009; Arcizet et al., 2011). Visual salience is reflected by the activity level evoked by individual objects, and a winner-take-all competition mediated by lateral inhibitory organization on this map determines the location of the strongest activity as the location to be attended to (Koch and Ullman, 1985; Itti and Koch, 2000). In these models, salience is coded only by response strength. However, from a theoretical standpoint, response onset latency may also play an important role. Under winner-take-all competition, earlier onset activities have an advantage in developing their activities. Namely, visual signals evoked by high-luminance objects can more rapidly arrive at PPC and suppress other later-onset activities evoked by low-luminance objects. Thus, the observed monotonic coding of luminance with latency could be crucial for the formation of a salience map with lateral inhibitory interactions, which are actually found in LIP (Falkner et al., 2010).

Link between visual activity and saccadic reaction time

Bell et al. (2006) recorded neuronal activity from the SC intermediate-layers while monkeys performed a visual detection task using a target with varying luminance levels. They showed that the onset of visual responses was earlier and saccadic reaction time was shorter with the higher-luminance target. Furthermore, Marino et al. (2012) found that peak magnitude and onset latency of visual response of SC neurons were strongly correlated with saccadic reaction time, highlighting a link between the initial SC visual activity and saccadic reaction time. We similarly found that luminance-related changes in response strength (post-latency and peak strengths) and response onset latency were significantly correlated with changes in saccadic reaction time (Fig. 7). We speculate that these luminance-dependent response changes may propagate into the saccade generation circuit, leading to changes in saccadic reaction time. Perhaps our findings are not surprising. Because LIP and SC receive rich visual signals from many common visual areas (LIP: Andersen et al., 1990; Blatt et al., 1990; Lewis and Van Essen, 2000; SC: Fries, 1984; Lock et al., 2003) and because LIP and SC are densely interconnected (Paré and Wurtz, 1997; Clower et al., 2001; Wurtz et al., 2001; Ferraina et al., 2002), the luminance-related properties of the visual response could be similar between PPC and SC, and this may produce a significant correlation between the visual response and saccadic reaction time in both areas.

Because only one stimulus was presented as a target in the current experiment, PPC neurons were capable of specifying the target position after visual response onset. To generate a saccade to that target, PPC neurons have only to send the position information to the downstream saccade preparation and generation circuits. Therefore, it is expected that

the length of time between visual response onset and saccade onset would be constant. However, the actual length of time was not constant but instead gradually increased as stimulus luminance decreased (Fig. 8), suggesting the existence of other luminance-dependent processing that contributes to the saccade generation. The fact that darker stimuli (weaker sensory signals) required longer time to generate a saccade reminds us of the accumulation and threshold model that was proposed to explain the neuronal process involved in decision making (Roitman and Shadlen, 2002; Gold and Shadlen, 2007). However, we found no clear common threshold in the activity of our samples (Fig. 5). Thus, if such a process exists, it may lie downstream and/or in parallel pathways (i.e., other areas not examined in this study such as FEF/SC and other PPC neuronal populations).

Previous studies using a visual search task showed that the activity of LIP neurons is stronger when the target appears in the receptive field than when a distractor appears in the receptive field (Ipata et al., 2006; Thomas and Paré, 2007; Balan et al., 2008; Ogawa and Komatsu, 2009). More importantly, the variability in target discrimination time at which neurons significantly discriminate the target from distractors in their activity accounts for the variability in saccadic reaction times (Ipata et al., 2006; Thomas and Paré, 2007), suggesting a link between LIP neuronal activity and saccade generation during visual search. A similar covariance with saccadic reaction time was found in FEF and SC (Sato et al., 2001; McPeek & Keller, 2002; Cohen et al., 2009; Shen et al., 2011). Although visual search and visual detection tasks differ in visual stimuli used and in task difficulty, both tasks ultimately demand that animals specify the target location and make a saccade to that location. As described before, because only one stimulus was presented as a target in

the visual detection task, PPC neurons may be capable of specifying the target position after the response onset. That is, the response onset time in a visual detection task may functionally correspond to the target discrimination time in a visual search task. However, we found only weak covariance between response onset latencies and saccadic reaction times (Fig. 9), suggesting that LIP differentially contributes to the generation of saccades in visual detection and visual search tasks. This view is supported by results of a previous inactivation study. Wardak et al. (2002) showed that muscimol-induced reversible inactivation of LIP had no effect on saccadic reaction time or the accuracy of saccades to a single target in either visually guided or memory-guided saccade tasks (but see Li et al., 1999), whereas serious deficits were observed in a visual search task. Thus, our result was consistent with the previous result.

In conclusion, we found a significant correlation between luminance-related changes in response strength/response onset latency of PPC neurons and changes in saccadic reaction time. However, the results of our additional analyses suggest that these response variables of PPC activity may be intermediate-stage variables and contribute less directly to saccade generation itself during visual detection.

Acknowledgements

The authors gratefully acknowledge the continuous support and encouragement of Prof. Kenji Kawano and valuable comments on an earlier manuscript by Kenichiro Miura and anonymous reviewers. We also acknowledge Nihon University and the National Bio-Resource Center for supplying the monkeys used in the present study. This work was supported by grants from the Ministry of Education, Culture, Sports, Science and Technology (MEXT) of Japan (#20500283).

References

Andersen, R.A., Asanuma, C., Essick, G. & Siegel, R.M. (1990) Corticocortical connections of anatomically and physiologically defined subdivisions within the inferior parietal lobule. *J Comp Neurol*, **296**, 65-113.

Arcizet, F., Mirpour, K. & Bisley, J.W. (2011) A pure salience response in posterior parietal cortex. *Cereb Cortex*, **21**, 2498-2506.

Balan, P.F., Oristaglio, J., Schneider, D.M. & Gottlieb, J. (2008) Neuronal correlates of the set-size effect in monkey lateral intraparietal area. *PLoS Biol*, **6**, e158.

Barash, S., Bracewell, R.M., Fogassi, L., Gnadt, J.W. & Andersen, R.A. (1991a) Saccade-related activity in the lateral intraparietal area. I. Temporal properties; comparison with area 7a. *J Neurophysiol*, **66**, 1095-1108.

Barash, S., Bracewell, R.M., Fogassi, L., Gnadt, J.W. & Andersen, R.A. (1991b) Saccade-related activity in the lateral intraparietal area. II. Spatial properties. *J Neurophysiol*, **66**, 1109-1124.

Bell, A.H., Everling, S. & Munoz, D.P. (2000) Influence of stimulus eccentricity and direction on characteristics of pro- and antisaccades in non-human primates. *J Neurophysiol*, **84**, 2595-2604.

Bell, A.H., Meredith, M.A., Van Opstal, A.J. & Munoz, D.P. (2006) Stimulus intensity modifies saccadic reaction time and visual response latency in the superior colliculus. *Exp Brain Res*, **174**, Sep-53.

Bisley, J.W. & Goldberg, M.E. (2003) Neuronal activity in the lateral intraparietal area and spatial attention. *Science*, **299**, 81-86.

Bisley, J.W., Krishna, B.S. & Goldberg, M.E. (2004) A rapid and precise on-response in posterior parietal cortex. *J Neurosci*, **24**, 1833-1838.

Blatt, G.J., Andersen, R.A. & Stoner, G.R. (1990) Visual receptive field organization and cortico-cortical connections of the lateral intraparietal area (area LIP) in the macaque. *J Comp Neurol*, **299**, 421-445.

Boch, R., Fischer, B. & Ramsperger, E. (1984) Express-saccades of the monkey: reaction times versus intensity, size, duration, and eccentricity of their targets. *Exp Brain Res*, **55**, 223-231.

Clower, D.M., West, R.A., Lynch, J.C. & Strick, P.L. (2001) The inferior parietal lobule is

the target of output from the superior colliculus, hippocampus, and cerebellum. *J Neurosci*, **21**, 6283-6291.

Cohen, J.Y., Heitz, R.P., Woodman, G.F. & Schall, J.D. (2009) Neural basis of the set-size effect in frontal eye field: timing of attention during visual search. *J Neurophysiol*, **101**, 1699-1704.

Colby, C.L., Duhamel, J.R. & Goldberg, M.E. (1996) Visual, presaccadic, and cognitive activation of single neurons in monkey lateral intraparietal area. *J Neurophysiol*, **76**, 2841-2852.

Crowder, N.A., Price, N.S., Mustari, M.J. & Ibbotson, M.R. (2009) Direction and contrast tuning of macaque MSTd neurons during saccades. *J Neurophysiol*, **101**, 3100-3107.

Doma, H. & Hallett, P.E. (1988) Dependence of saccadic eye-movements on stimulus luminance, and an effect of task. *Vision Res*, **28**, 915-924.

Efron, B. & Tibshirani, R.J. (1993) *An Introduction to the Bootstrap*. Chapman & Hall, New York.

Falkner, A.L., Krishna, B.S. & Goldberg, M.E. (2010) Surround suppression sharpens the priority map in the lateral intraparietal area. *J Neurosci*, **30**, 12787-12797.

Ferraina, S., Paré, M. & Wurtz, R.H. (2002) Comparison of cortico–cortical and cortico–collicular signals for the generation of saccadic eye movements. *J Neurophysiol*, **87**, 845-858.

Foley, J.M., Varadharajan, S., Koh, C.C. & Farias, M.C. (2007) Detection of Gabor patterns of different sizes, shapes, phases and eccentricities. *Vision Res*, **47**, 85-107.

Fries, W. (1984) Cortical projections to the superior colliculus in the macaque monkey: a retrograde study using horseradish peroxidase. *J Comp Neurol*, **230**, 55-76.

Fuchs, A.F. & Robinson, D.A. (1966) A method for measuring horizontal and vertical eye movement chronically in the monkey. *J Appl Physiol*, **21**, 1068-1070.

Gawne, T.J. (2000) The simultaneous coding of orientation and contrast in the responses of V1 complex cells. *Exp Brain Res*, **133**, 293-302.

Gawne, T.J., Kjaer, T.W. & Richmond, B.J. (1996) Latency: another potential code for feature binding in striate cortex. *J Neurophysiol*, **76**, 1356-1360.

Gifford, G.W., 3rd & Cohen, Y.E. (2004) Effect of a central fixation light on auditory

spatial responses in area LIP. *J Neurophysiol*, **91**, 2929-2933.

Gnadt, J.W. & Andersen, R.A. (1988) Memory related motor planning activity in posterior parietal cortex of macaque. *Exp Brain Res*, **70**, 216-220.

Gold, J.I. & Shadlen, M.N. (2007) The neural basis of decision making. *Annu Rev Neurosci*, **30**, 535-574.

Gottlieb, J.P., Kusunoki, M. & Goldberg, M.E. (1998) The representation of visual salience in monkey parietal cortex. *Nature*, **391**, 481-484.

Hikosaka, O. & Wurtz, R.H. (1983) Visual and oculomotor functions of monkey substantia nigra pars reticulata. III. Memory-contingent visual and saccade responses. *J Neurophysiol*, **49**, 1268-1284.

Hughes, H.C. & Kelsey, J.V. (1984) Response-dependent effects on near-threshold detection performance: saccades versus manual responses. *Percept Psychophys*, **35**, 543-546.

Ipata, A.E., Gee, A.L., Goldberg, M.E. & Bisley, J.W. (2006) Activity in the lateral intraparietal area predicts the goal and latency of saccades in a free-viewing visual search task. *J Neurosci*, **26**, 3656-3661.

Itti, L. & Koch, C. (2000) A saliency-based search mechanism for overt and covert shifts of visual attention. *Vision Res*, **40**, 1489-1506.

Jaśkowski, P. & Sobieralska, K. (2004) Effect of stimulus intensity on manual and saccadic reaction time. *Percept Psychophys*, **66**, 535-544.

Judge, S.J., Richmond, B.J. & Chu, F.C. (1980) Implantation of magnetic search coils for measurement of eye position: an improved method. *Vision Res*, **20**, 535-538.

Kiorpes, L. & Kiper, D.C. (1996) Development of contrast sensitivity across the visual field in macaque monkeys (Macaca nemestrina). *Vision Res*, **36**, 239-247.

Koch, C. & Ullman, S. (1985) Shifts in selective visual attention: towards the underlying neural circuitry. *Hum Neurobiol*, **4**, 219-227.

Lawrence, B.M., White, R.L., 3rd & Snyder, L.H. (2005) Delay-period activity in visual, visuomovement, and movement neurons in the frontal eye field. *J Neurophysiol*, **94**, 1498-1508.

Lee, J., Williford, T. & Maunsell, J.H. (2007) Spatial attention and the latency of neuronal responses in macaque area V4. *J Neurosci*, **27**, 9632-9637.

Lee, J., Kim, H.R. & Lee, C. (2010) Trial-to-trial variability of spike response of V1 and saccadic response time. *J Neurophysiol*, **104**, 2556-2572.

Lewis, J.W. & Van Essen, D.C. (2000) Corticocortical connections of visual, sensorimotor, and multimodal processing areas in the parietal lobe of the macaque monkey. *J Comp Neurol*, **428**, 112-137.

Li, C.S., Mazzoni, P. & Andersen, R.A. (1999) Effect of reversible inactivation of macaque lateral intraparietal area on visual and memory saccades. *J Neurophysiol*, **81**, 1827-1838.

Linden, J.F., Grunewald, A. & Andersen, R.A. (1999) Responses to auditory stimuli in macaque lateral intraparietal area. II. Behavioral modulation. *J Neurophysiol*, **82**, 343-358.

Lock, T.M., Baizer, J.S. & Bender, D.B. (2003) Distribution of corticotectal cells in macaque. *Exp Brain Res*, **151**, 455-470.

Maimon, G. & Assad, J.A. (2006) A cognitive signal for the proactive timing of action in macaque LIP. *Nat Neurosci*, **9**, 948-955.

Marino, R.A. & Munoz, D.P. (2009) The effects of bottom-up target luminance and top-down spatial target predictability on saccadic reaction times. *Exp Brain Res*, **197**, 321-335.

Marino, R.A., Levy, R., Boehnke, S., White, B.J., Itti, L. & Munoz, D.P. (2012) Linking visual response properties in the superior colliculus to saccade behavior. *Eur J Neurosci*, **35**, 1738-1752.

Maunsell, J.H. & Gibson, J.R. (1992) Visual response latencies in striate cortex of the macaque monkey. *J Neurophysiol*, **68**, 1332-1344.

McPeek, R.M. & Keller, E.L. (2002) Saccade target selection in the superior colliculus during a visual search task. *J Neurophysiol*, **88**, 2019-2034.

Mountcastle, V.B., Lynch, J.C., Georgopoulos, A., Sakata, H. & Acuna, C. (1975) Posterior parietal association cortex of the monkey: command functions for operations within extrapersonal space. *J Neurophysiol*, **38**, 871-908.

Nakamura, K., Matsumoto, K., Mikami, A. & Kubota, K. (1994) Visual response properties of single neurons in the temporal pole of behaving monkeys. *J Neurophysiol*, **71**, 1206-1221.

Ogawa, T. & Komatsu, H. (2009) Condition-dependent and condition-independent target selection in the macaque posterior parietal cortex. *J Neurophysiol*, **101**, 721-736.

Paré, M. & Wurtz, R.H. (1997) Monkey posterior parietal cortex neurons antidromically activated from superior colliculus. *J Neurophysiol*, **78**, 3493-3497.

Petersch, B., Bogner, J., Fransson, A., Lorang, T. & Potter, R. (2004) Effects of geometric distortion in 0.2T MRI on radiotherapy treatment planning of prostate cancer. *Radiother Oncol*, **71**, 55-64.

Pointer, J.S. & Hess, R.F. (1989) The contrast sensitivity gradient across the human visual field: with emphasis on the low spatial frequency range. *Vision Res*, **29**, 1133-1151.

Price, N.S., Crowder, N.A., Hietanen, M.A. & Ibbotson, M.R. (2006) Neurons in V1, V2, and PMLS of cat cortex are speed tuned but not acceleration tuned: the influence of motion adaptation. *J Neurophysiol*, **95**, 660-673.

Richmond, B.J., Optican, L.M., Podell, M. & Spitzer, H. (1987) Temporal encoding of two-dimensional patterns by single units in primate inferior temporal cortex. I. Response characteristics. *J Neurophysiol*, **57**, 132-146.

Robson, J.G. & Graham, N. (1981) Probability summation and regional variation in contrast sensitivity across the visual field. *Vision Res*, **21**, 409-418.

Roitman, J.D. & Shadlen, M.N. (2002) Response of neurons in the lateral intraparietal area during a combined visual discrimination reaction time task. *J Neurosci*, **22**, 9475-9489.

Sato, T., Murthy, A., Thompson, K.G. & Schall, J.D. (2001) Search efficiency but not response interference affects visual selection in frontal eye field. *Neuron*, **30**, 583-591.

Schall, J.D., Morel, A., King, D.J. & Bullier, J. (1995) Topography of visual cortex connections with frontal eye field in macaque: convergence and segregation of processing streams. *J Neurosci*, **15**, 4464-4487.

Schmolesky, M.T., Wang, Y., Hanes, D.P., Thompson, K.G., Leutgeb, S., Schall, J.D. & Leventhal, A.G. (1998) Signal timing across the macaque visual system. *J Neurophysiol*, **79**, 3272-3278.

Shadlen, M.N. & Newsome, W.T. (2001) Neural basis of a perceptual decision in the parietal cortex (area LIP) of the rhesus monkey. *J Neurophysiol*, **86**, 1916-1936.

Shen, K., Valero, J., Day, G.S. & Paré, M. (2011) Investigating the role of the superior

colliculus in active vision with the visual search paradigm. *Eur J Neurosci*, **33**, 2003-2016.

Snyder, L.H., Batista, A.P. & Andersen, R.A. (1997) Coding of intention in the posterior parietal cortex. *Nature*, **386**, 167-170.

Thomas, N.W. & Paré, M. (2007) Temporal processing of saccade targets in parietal cortex area LIP during visual search. *J Neurophysiol*, **97**, 942-947.

Thompson, K.G., Hanes, D.P., Bichot, N.P. & Schall, J.D. (1996) Perceptual and motor processing stages identified in the activity of macaque frontal eye field neurons during visual search. *J Neurophysiol*, **76**, 4040-4055.

Wardak, C., Olivier, E. & Duhamel, J.R. (2002) Saccadic target selection deficits after lateral intraparietal area inactivation in monkeys. *J Neurosci*, **22**, 9877-9884.

Wolfe, J.M. (1994) Guided search 2.0: a revised model of visual search. *Psychonomic Bulletin & Review*, **1**(2): 202-238

Wurtz, R.H., Sommer, M.A., Paré, M. & Ferraina, S. (2001) Signal transformations from cerebral cortex to superior colliculus for the generation of saccades. *Vision Res*, **41**, 3399-3412.

Figure Legends

Figure 1. Experimental design and behavioral performance.

A: Visual stimulation sequence employed during a reaction-time visual detection task. After fixation on a central spot (1,000 ms or 1,500–2,000 ms), a target stimulus with five luminance levels appeared at one of two peripheral locations. One was located in the receptive field of a recorded neuron, and the other was located diametrically opposite from the fixation point. Monkeys had to detect the target stimulus and make a saccade to it. The target stimulus and the fixation spot were removed when a saccade was detected on-line by a computer. If the saccade was performed correctly, another spot reappeared at the target location. The monkey received a liquid reward after fixating on that spot for 600 ms. ITI, inter-trial interval; SRT, saccadic reaction time. ***B, C***: Mean correct performance (***B***) and mean saccadic reaction time (***C***) at five luminance levels collapsed across recording sessions. Data are plotted as a function of stimulus contrast as well as luminance. Error bars indicate SD across recording sessions.

Figure 2. Magnetic resonance images of recording sites from one monkey.

A: A three-dimensional view of the brain of one monkey. Five bright rods in the right hemisphere indicate hollow tubes filled with a glycerin solution, which were embedded in a plastic base attached to the recording chamber. These tubes served as position reference markers. The bright mass located at the foot of the tubes was an ointment with which a hole in the skull was filled to protect the dura matter surface. ***B***: Penetration sites on the cortical

surface. Large circles indicate the sites defined by extensions from the reference tubes. The penetration sites where neurons were recorded (small circles) were reconstructed with the coordinate determined by the reference tubes. The black outline indicates the outline of the skull hole. ***C***: The number of neurons recorded within each grid location. The thick gray line indicates the location of the intraparietal sulcus (IPS). ***D***: Reconstruction of the recording zone in the planes that were sectioned parallel to the penetrations at two levels (*line* 1 and 2 in ***B***). The arrowheads next to IPS represent the location boundaries from which neurons were recorded. ***E***: Coronal slices representing recording positions from the most anterior to the most posterior. The A–P levels are indicated at the top of each image. CS, central sulcus; IPS, intraparietal sulcus.

Figure 3. Activity of a PPC neuron during a visual detection task.

A: The activity of a visually responsive neuron in response to five luminance levels. Solid and dashed curves in each panel indicate the spike density functions (mean ± SEM) observed when the target appeared in the receptive field and away from it, respectively. Traces were smoothed with a Gaussian function (SD = 3 ms) and are aligned at the time of stimulus presentation (left panel), response onset latency (middle panel), or saccade initiation (right panel). Rectangles, gray vertical lines, and numbers indicate the times (ms) at which response onsets were assigned. Circles indicate the peaks in activity. Raster plots (colored ticks) and saccadic reaction times (black ticks) for individual trials are shown above the spike density functions. The upper half indicates trials in which the target appeared in the receptive field, and the lower half indicates the trials in which the target

appeared away from the receptive field. The mean saccadic reaction time during each stimulus condition is indicated by a triangle with a number above it. ***B***: The spike density functions obtained from the five luminance levels are superimposed and are shown for ease of comparison. Gray horizontal lines indicate the response onset latency threshold calculated using the Poisson distribution.

Figure 4. Response strength and response onset latency at different luminance levels for the PPC neuron shown in Fig. 3.

Post-latency strength calculated from the 50-ms activity after response onset (***A***), peak strength (***B***), and response onset latency (***C***) is illustrated as a function of stimulus luminance. Error bars indicate 95% confidence intervals. The stimulus contrast is indicated along the upper horizontal axis, and the stimulus luminance along the lower horizontal axis.

Figure 5. Population average responses of PPC visual neurons.

Population average spike density functions constructed by averaging the spike density functions across neurons (n = 43) for each luminance condition. The responses were computed for trials in which the target appeared in the receptive field. Traces in each panel are aligned at the time of stimulus presentation (left panel), response onset (middle panel), or saccade onset (right panel). Mean saccadic reaction times are indicated by triangles at the individual luminance level.

Figure 6. Population analyses of luminance-related changes in response strength and response onset latency.

Post-latency strength (***A***), peak strength (***B***), and response onset latency (***C***) for all PPC neurons (n = 43) are illustrated as a function of stimulus luminance. Gray circles connected with a thin line represent response strengths or latencies obtained from each neuron. Black circles connected with a thick line and vertical bars indicate the mean ± SD. The gray line indicates the linear regression line. Post-latency strength and peak strength were normalized so that the mean value across the five luminance levels is 1 for each neuron.

Figure 7. Relationship between response strength/response onset latency and saccadic reaction time.

Saccadic reaction time is plotted as a function normalized post-latency strength (***A***), normalized peak strength (***B***), and response onset latency (***C***). Small symbols indicate values obtained from each neuron under each luminance condition. Different luminance conditions are indicated by different symbols. Large symbols connected with a thick line indicate the mean of all neurons (n = 43) for each luminance condition. Gray lines indicate the linear regression lines.

Figure 8. Distribution of neuronal–saccade onset delay.

Distributions of the length of time between the response onset and the saccade onset are shown separately for each stimulus luminance. Vertical dotted lines indicate mean values for each stimulus condition. SRT, saccadic reaction time.

Figure 9. Relationship between variability in initial visual response and variability in saccadic reaction time.

A-C: Relationship of variability in saccadic reaction time with variability in normalized post-latency strength (***A***), in normalized peak strength (***B***), and in response onset latency (***C***). Individual plots indicate values obtained from each neuron under each luminance condition. Different luminance conditions are indicated by different symbols. ***C***: The solid gray line indicates the regression line, which was forced to pass through the origin. Its slope was significantly greater than 0 (regression slope = 0.10, $p < 0.01$). The dotted oblique line is the line of unity. ***D***: The slope values when the regression line was separately fitted to the data points for each luminance level. In all cases, the slope values were positive (0.028–0.15) but not significantly different from zero (regression slope, $p > 0.05$).

Table 1. Effect of target luminance on saccadic dynamics.

The mean values for saccade peak velocity, duration, amplitude, and endpoint error collapsed across 43 recording sessions are shown for each stimulus luminance. The *p*-values (one-way repeated-measures ANOVA) are shown in the right-most column.

	Stimulus luminance (cd/m^2)						
	20.6	2.47	1.02	0.90	0.83	*F* statistics	*p*
Saccade peak velocity (degree/s)	420	418	409	400	397	$F_{4,168} = 133$	< 0.001
Saccade duration (ms)	37.3	37.5	38.4	39.2	39.6	$F_{4,168} = 29.4$	< 0.001
Saccade amplitude (degree)	8.13	8.14	8.09	8.04	8.03	$F_{4,168} = 13.6$	< 0.001
Saccade endpoint error (degree)	0.68	0.60	0.61	0.64	0.69	$F_{4,168} = 2.77$	< 0.05

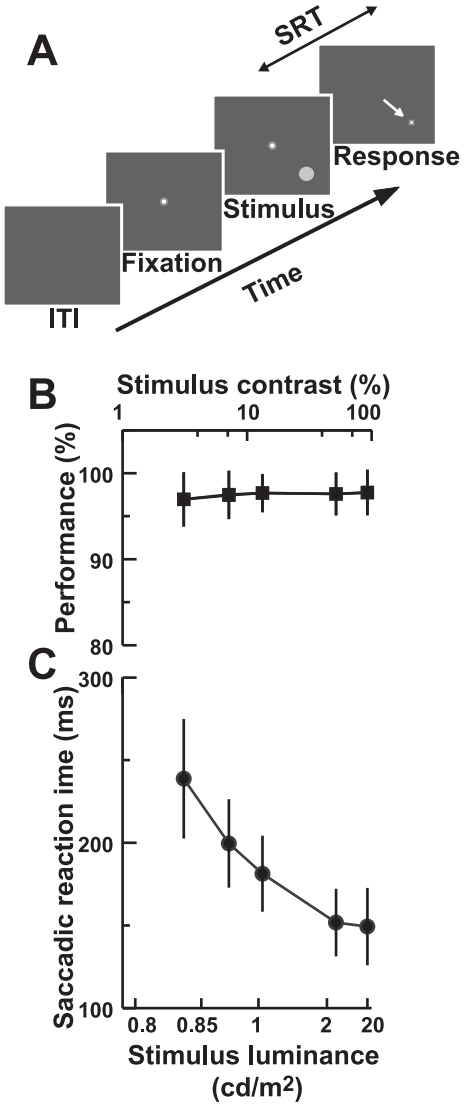
A
SRT
Response
Stimulus
Fixation
ITI
Time
B
Stimulus contrast (%)
1
10
100
Performance (%)
100
90
80
C
Saccadic reaction ime (ms)
300
200
100
0.8
0.85
1
2
20
Stimulus luminance
(cd/m2)

Fig. 1

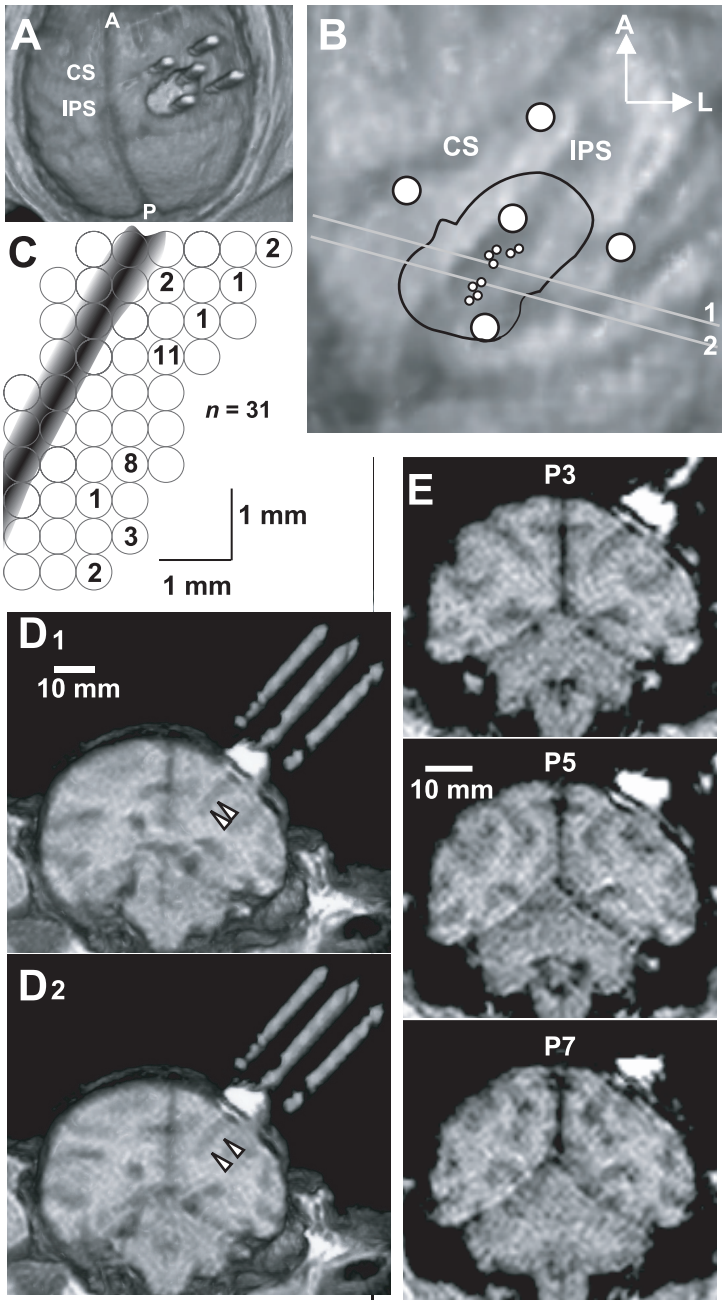
A
A
CS
IPS
P
B
A
L
CS
IPS
1
2
C
2
2
1
1
11
n = 31
8
1
3
2
1 mm
1 mm
D1
10 mm
D2
E
P3
P5
10 mm
P7

Fig. 2

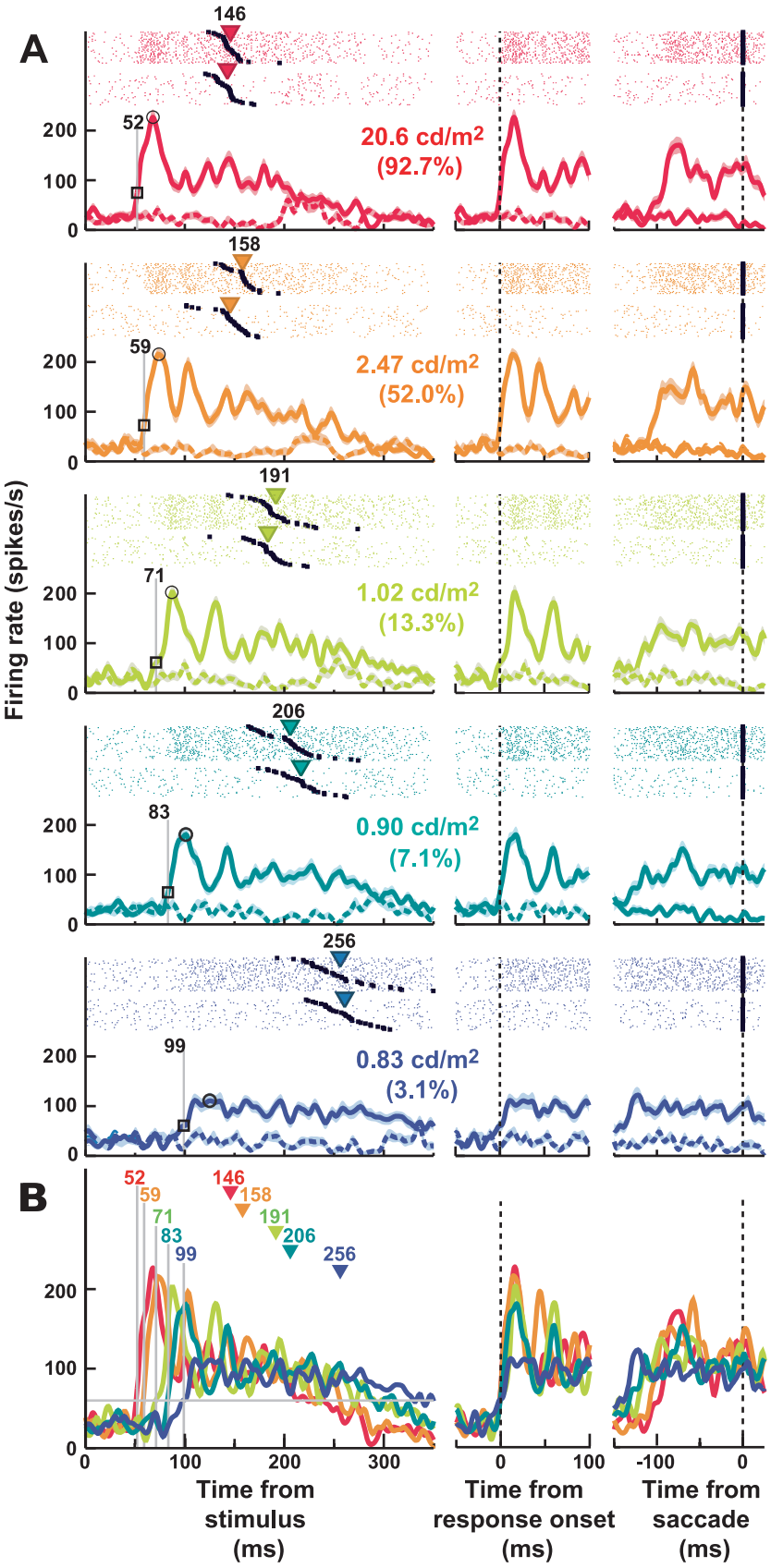
A
146
52
20.6 cd/m2
(92.7%)
158
59
2.47 cd/m2
(52.0%)
191
71
1.02 cd/m2
(13.3%)
206
83
0.90 cd/m2
(7.1%)
256
99
0.83 cd/m2
(3.1%)
Firing rate (spikes/s)
B
52
59
71
83
99
146
158
191
206
256
0
100
200
300
-100
Time from stimulus (ms)
Time from response onset (ms)
Time from saccade (ms)

Fig. 3

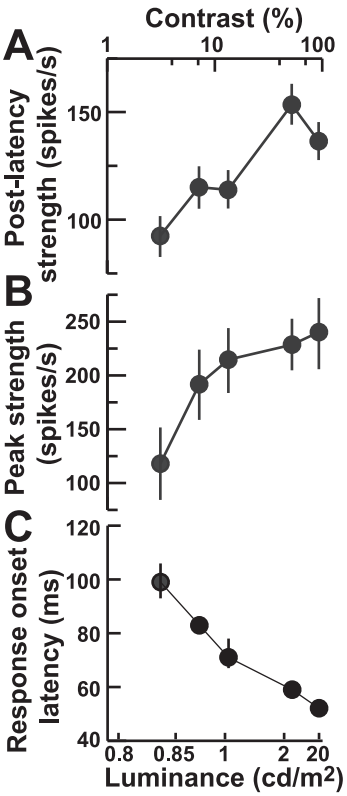
A
Contrast (%)
1
10
100
Post-latency strength (spikes/s)
150
100
B
Peak strength (spikes/s)
250
200
150
100
C
Response onset latency (ms)
120
100
80
60
40
0.8
0.85
1
2
20
Luminance (cd/m2)

Fig. 4

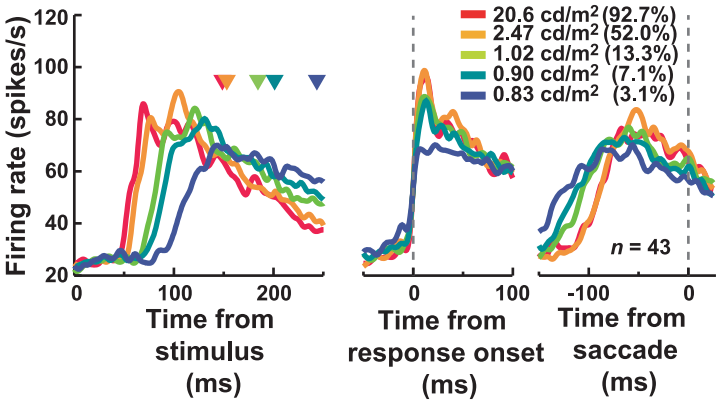
Firing rate (spikes/s)
120
100
80
60
40
20
0
100
200
Time from stimulus (ms)
20.6 cd/m² (92.7%)
2.47 cd/m² (52.0%)
1.02 cd/m² (13.3%)
0.90 cd/m² (7.1%)
0.83 cd/m² (3.1%)
0
100
Time from response onset (ms)
n = 43
-100
0
Time from saccade (ms)

Fig. 5

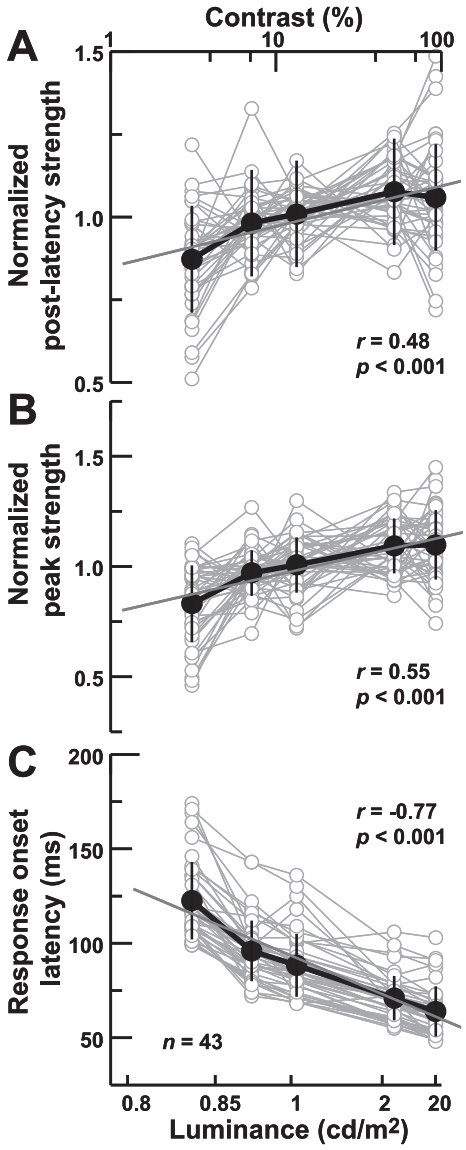
A
Contrast (%)
1
10
100
1.5
1.0
0.5
Normalized post-latency strength
r = 0.48
p < 0.001
B
Normalized peak strength
1.5
1.0
0.5
r = 0.55
p < 0.001
C
Response onset latency (ms)
200
150
100
50
r = -0.77
p < 0.001
n = 43
0.8
0.85
1
2
20
Luminance (cd/m2)

Fig. 6

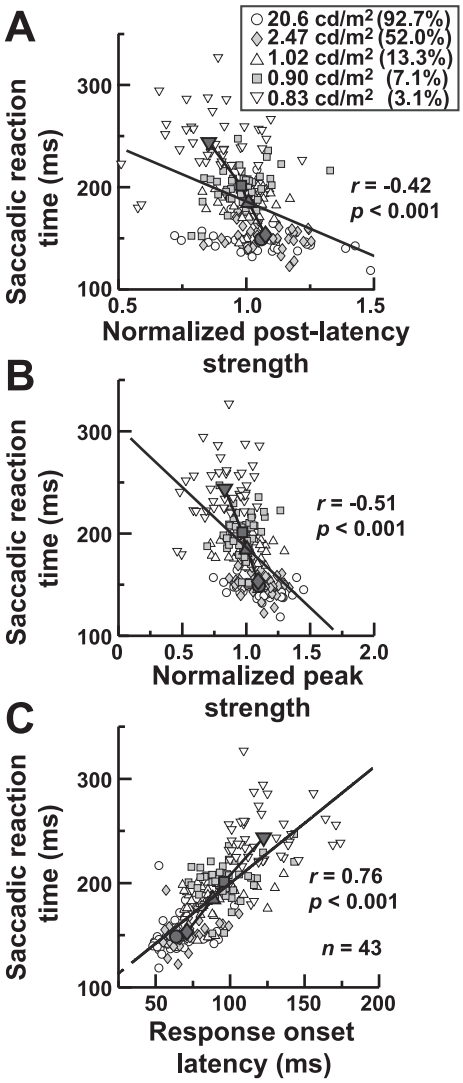
A
20.6 cd/m² (92.7%)
2.47 cd/m² (52.0%)
1.02 cd/m² (13.3%)
0.90 cd/m² (7.1%)
0.83 cd/m² (3.1%)
r = -0.42
p < 0.001
Saccadic reaction time (ms)
Normalized post-latency strength
B
r = -0.51
p < 0.001
Saccadic reaction time (ms)
Normalized peak strength
C
r = 0.76
p < 0.001
n = 43
Saccadic reaction time (ms)
Response onset latency (ms)

Fig. 7

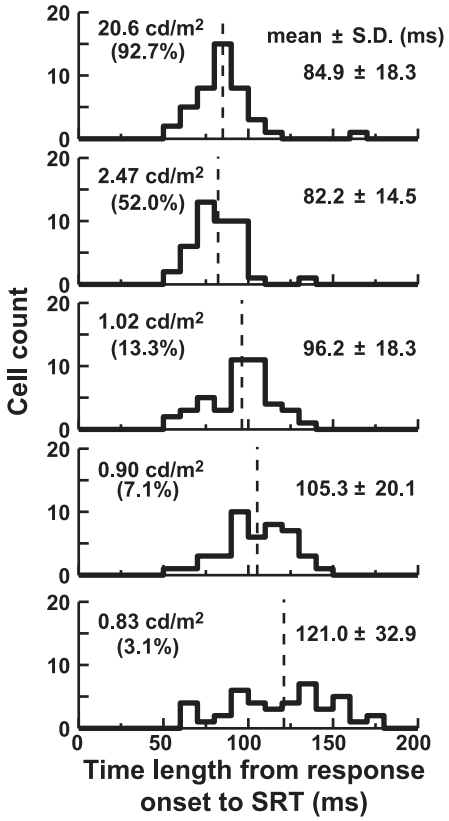
20.6 cd/m2
(92.7%)
mean ± S.D. (ms)
84.9 ± 18.3
2.47 cd/m2
(52.0%)
82.2 ± 14.5
1.02 cd/m2
(13.3%)
96.2 ± 18.3
0.90 cd/m2
(7.1%)
105.3 ± 20.1
0.83 cd/m2
(3.1%)
121.0 ± 32.9
Cell count
0
10
20
0
50
100
150
200
Time length from response
onset to SRT (ms)

Fig. 8

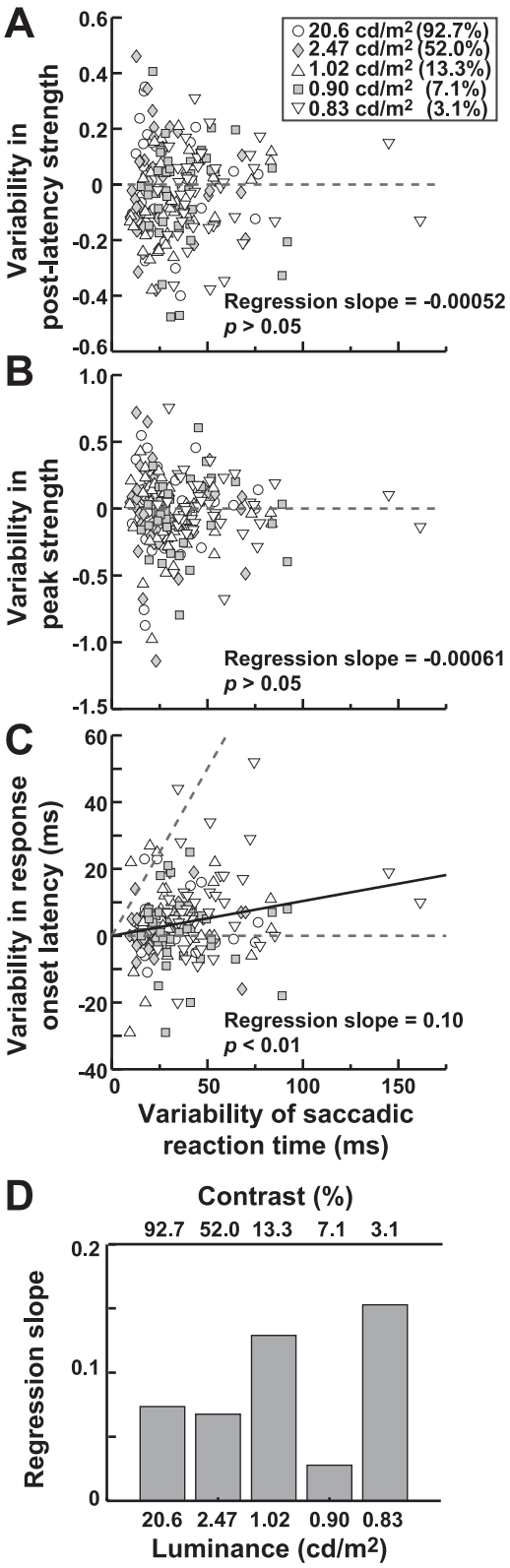
A
20.6 cd/m2 (92.7%)
2.47 cd/m2 (52.0%)
1.02 cd/m2 (13.3%)
0.90 cd/m2 (7.1%)
0.83 cd/m2 (3.1%)
Variability in post-latency strength
Regression slope = -0.00052
p > 0.05
B
Variability in peak strength
Regression slope = -0.00061
p > 0.05
C
Variability in response onset latency (ms)
Regression slope = 0.10
p < 0.01
Variability of saccadic reaction time (ms)
D
Contrast (%)
92.7 52.0 13.3 7.1 3.1
Regression slope
20.6 2.47 1.02 0.90 0.83
Luminance (cd/m2)

Fig. 9